Received: 30 April 2021 | Revised: 22 July 2021 | Accepted: 22 July 2021

DOI: 10.1111/mpp.13117

ORIGINAL ARTICLE

Molecular Plant Pathology WILEY

Xanthomonas transcriptome inside cauliflower hydathodes reveals bacterial virulence strategies and physiological adaptations at early infection stages

Julien S. Luneau | Aude Cerutti | Brice Roux | Sébastien Carrère | Marie-Françoise Jardinaud | Antoine Gaillac | Carine Gris | Emmanuelle Lauber | Richard Berthomé | Matthieu Arlat | Alice Boulanger | Laurent D. Noël

LIPME, Université de Toulouse, INRAE, CNRS, Université Paul Sabatier, Castanet-Tolosan, France

Present address: Brice Roux, HalioDx, Luminy Biotech Entreprises, Marseille Cedex 9, France

Correspondence
Alice Boulanger and Laurent Noël, LIPME, Université de Toulouse, INRAE, CNRS, Université Paul Sabatier, Castanet-Tolosan, France.
Emails: alice.boulanger@inrae.fr; laurent.noel@inrae.fr

Funding information
Labex, Grant/Award Number: TULIP ANR-10-LABX-41 and ANR-11-IDEX-0002-02; European Cooperation in Science and Technology, Grant/Award Number: CA16107 EuroXanth; Agence Nationale de la Recherche, Grant/Award Number: NEPHRON (ANR-18-CE20-0020-01), XANTHOMIX (ANR-2010-GENM-013-02), XBOX (ANR-19-CE20-JCJC-0014-01) and Xopaque (ANR-10-JCJC-1703-01)

Abstract

Xanthomonas campestris pv. *campestris* (Xcc) is a seed-transmitted vascular pathogen causing black rot disease on cultivated and wild Brassicaceae. Xcc enters the plant tissues preferentially via hydathodes, which are organs localized at leaf margins. To decipher both physiological and virulence strategies deployed by Xcc during early stages of infection, the transcriptomic profile of Xcc was analysed 3 days after entry into cauliflower hydathodes. Despite the absence of visible plant tissue alterations and despite a biotrophic lifestyle, 18% of Xcc genes were differentially expressed, including a striking repression of chemotaxis and motility functions. The Xcc full repertoire of virulence factors had not yet been activated but the expression of the HrpG regulon composed of 95 genes, including genes coding for the type III secretion machinery important for suppression of plant immunity, was induced. The expression of genes involved in metabolic adaptations such as catabolism of plant compounds, transport functions, sulphur and phosphate metabolism was upregulated while limited stress responses were observed 3 days postinfection. We confirmed experimentally that high-affinity phosphate transport is needed for bacterial fitness inside hydathodes. This analysis provides information about the nutritional and stress status of bacteria during the early biotrophic infection stages and helps to decipher the adaptive strategy of Xcc to the hydathode environment.

KEYWORDS

adaptation, *hrp* gene cluster, *hrpG*, hydathode, transcriptome, type III effector, type III secretion

Julien S. Luneau and Aude Cerutti contributed equally to this work.

1 | INTRODUCTION

Xanthomonas campestris pv. *campestris* (Xcc) is a seed-transmitted vascular pathogen causing black rot disease on Brassicaceae. This bacterium has a complex lifestyle composed of both epiphytic and endophytic stages (Vicente & Holub, 2013) that have been studied using molecular genetics since the 1980s (Daniels et al., 1984). Xcc epiphytic life is associated with environmental stresses such as UV light or dehydration and relies, for instance, on the production of xanthan exopolysaccharides (EPS) or protective pigments such as xanthomonadin. Upon favourable conditions, Xcc will gain access into the leaf inner tissues via wounds or hydathodes (Cerutti et al., 2017).

Hydathodes are plant organs mediating guttation localized at the leaf margin. Hydathodes are classically composed of an epidermis with water pores resembling stomata and an inner loose parenchyma called epithem irrigated by numerous xylem vessels (Cerutti et al., 2019). These specific structures offer an ecological niche for pathogenic bacteria and a rapid access to xylem vessels leading to systemic vascular infections (Cerutti et al., 2017). However, only a few pathogens have been demonstrated to colonize this niche and the conditions driving hydathode infection are poorly understood (Carlton et al., 1998; Cerutti et al., 2017; Fukui et al., 1996; Hugouvieux et al., 1998; Nino-Liu et al., 2006; Robene-Soustrade et al., 2006). While there is no evidence of a preinvasive immunity limiting Xcc entry through water pores, a postinvasive immunity was described inside the epithem (Cerutti et al., 2017). This is best revealed by the inability of a bacterial mutant of the hypersensitive response and pathogenicity (Hrp) type III secretion (T3S) system to multiply in the epithem and to initiate vascular infections (Cerutti et al., 2017). The T3S system is responsible for the secretion and translocation of type III effector (T3E) proteins inside plant cells, where they interfere with plant physiology and suppress plant immunity (Buttner & Bonas, 2010). These results highlight the importance of immune suppression for the establishment of the infection.

Once inside hydathodes, Xcc adapts to this niche and adopts a biotrophic lifestyle: bacteria slowly multiply in the apoplastic spaces between epithem cells without causing visible tissue alterations as observed until 3 days postinfection (dpi) of cauliflower hydathodes (Cerutti et al., 2017). A switch to a necrotrophic behaviour is then observed, resulting in the almost complete digestion of the epithem at 6 dpi and Xcc vascularization. Systemic infection reaching the flowers will cause seed colonization and transmission to seedlings (Darsonval et al., 2009; Dutta et al., 2014).

During infection, Xcc may feed on guttation fluid, xylem sap or plant tissues (Duge de Bernonville et al., 2014). This process can be facilitated by high-affinity nutrient transport systems such as TonB-dependent transporters (TBDT) for mineral (e.g., iron) or carbohydrate nutrition (e.g., sucrose; Blanvillain et al., 2007) and a large repertoire of plant cell wall-degrading enzymes secreted through the type II secretion (T2S) system. Such metabolic adaptations need to be finely coordinated throughout the infectious cycle. Master regulators include the *rpf*-diffusible signal factor (DSF) quorum-sensing system, sensors of nutrient availability and metabolic activity and two-component systems. These regulation pathways allow bacterial cells to respond appropriately to diverse extracellular stimuli encountered during its life cycle, such as oxidative stress, oxygen levels, pH, temperature, and plant signals (He & Zhang, 2008; Qian et al., 2008; Tao et al., 2010). Among these regulators, some are well known to play a major role in virulence, such as the response regulator HrpG, which is, with the transcriptional regulator HrpX, the master regulator of the T3S regulon (Noël et al., 2001; Roux et al., 2015; Zhang et al., 2020).

Our knowledge of Xcc gene expression in planta remains elusive and technically challenging, especially at early stage of infection when bacterial populations are low. Indeed, most transcriptomic studies in Xcc or other *Xanthomonas* species have so far been performed in vitro focusing on specific regulons of the *hrpG* and *hrpX* genes in *hrp*-inducing media, of the *prc* protease gene, of the DSF-mediated quorum-sensing system, or of the *gum* genes responsible for xanthan production (Alkhateeb et al., 2016; An et al., 2014; Chen et al., 2018; Jalan et al., 2013; Kim et al., 2016; Li et al., 2019; Liao et al., 2016; Liu et al., 2013; Noh et al., 2016; Schmidtke et al., 2012; Zhang et al., 2013). Only a few in planta transcriptomic analyses have been performed on *Xanthomonas* (Getaz et al., 2020; Lee et al., 2017; Li et al., 2019; Liao et al., 2019) and all at late stages of infection and/or in comparison to in vitro-grown bacteria. Such in planta transcriptomic approaches would help identify new pathogenic behaviours and adaptation to the host during the infection process and in the different tissues colonized. Such approaches are also good descriptors of the environmental conditions and stresses imposed by the host on the bacterial pathogen (Nobori et al., 2018).

In this study, we compare the transcriptome of Xcc inside cauliflower hydathodes 4 or 72 hr after inoculation, that is, during the biotrophic stage of infection, to determine Xcc adaptative transcriptomic responses and infer the environmental conditions met by this bacterial pathogen inside hydathodes.

2 | RESULTS

2.1 | Improved annotation of Xcc strain 8004 genome based on a large transcriptomic data set

Transcriptomic analyses are intrinsically dependent on the proper structural annotation of genes. To improve annotation of the Xcc strain 8004 using experimental expression data, we produced the transcriptome of two nearly isogenic strains grown in MOKA medium: wildtype strain 8004 and strain 8004::*hrpG**, which expresses the constitutively active variant E44K of the *hrp* response regulator HrpG (Guy et al., 2013b) (see later for comparative analysis of the HrpG regulon). Total RNAs were extracted from exponentially growing bacteria and subjected to ribodepletion as described (Roux et al., 2015). Small (<200 nucleotides [nt]) and large (>200 nt) RNA

TABLE 1 Impact of transcriptomic data on the de novo annotation of *Xanthomonas campestris* pv. *campestris* (Xcc) strain 8004 genome

RNA-Seq data used[a]	All genes	mRNA[b]	rRNA[c] operon	tRNA[d]	Other ncRNA[e]	5′ UTR[f]	3′ UTR[g]	Reference	Accession number
No	4,333	4,273	2	53	1	–	–	Qian et al. (2005)	NCBI CP000050.1
No	4,631	4,478	2	54	93	–	–	NCBI	NCBI NC_007086.1
Yes	5,431	4,617	2	55	753	1724	1,246	This study	https://doi.org/10.25794/reference/id52ofys

[a]Use of merged transcriptomic datasets from *Xcc* strain 8004 derivatives (wild type or 8004::*hrpG**) grown in vitro in MOKA medium.
[b]Protein coding sequence.
[c]Ribosomal RNA.
[d]Transfer RNA.
[e]Noncoding RNA.
[f]5′ untranslated region.
[g]3′ untranslated region.

fractions were subjected to paired-end and single-end strand-specific sequencing, respectively. RNAs protected by a 5′ triphosphate group in the small RNA fraction were used to map precisely the transcriptional start sites. Those 13 libraries corresponding to 88,130,260 and 135,564,422 reads from small and large RNA fractions, respectively, were used to refine genomic annotation. More than 1,724 transcriptional starts (5′ untranslated regions [UTRs]) and 1,246 3′ UTRs could be experimentally defined (Table 1, https://dx.doi.org/10.25794/reference/id52ofys). The predicted translational start site was modified for 1,164 coding sequences (CDSs) and 753 small noncoding RNAs (ncRNAs) were evidenced. These results highlight the importance of experimentally supported genome annotations and offer improved resources for the functional analysis of Xcc transcriptome.

2.2 | Xcc transcriptome remodelling at early stages of hydathode infection

To capture a proxy of the physiological status of Xcc at the early stage of plant leaf infection, we performed RNA sequencing (RNA-Seq) on bacteria harvested from cauliflower hydathodes 72 hr after a rapid (15 s) dip inoculation of an attached leaf (Figure 1a). This 72 hr postinoculation (hpi) time point corresponds to a biotrophic phase of the infection where the bacteria are still limited to the epithemal apoplastic spaces (Cerutti et al., 2017). After 4 hr of continuous immersion of a detached leaf in the bacterial suspension (Figure 1a), c.10^5 cfu/hydathode is detected similar to the bacterial titres at 72 hpi (Figure S1). Calculation of sample-to-sample Euclidian distances indicated that the 4 hpi transcriptomes cluster with the 72 hpi timepoints rather than with in vitro samples (Figure S2a). This 4 hpi condition was thus chosen as the reference condition because it allows the narrow comparison of two bacterial populations in contact with plant tissues for 4 and 72 hr and a focus on bacterial adaptation to the plant environment. This 4 hpi condition cannot serve to analyse the changes occurring at the hydathode entry step because of the lack of reference transcriptomic data from bacteria coming from the initial inoculum. However, this timepoint is a relevant reference to investigate bacterial acclimation to the hydathode environment.

During hydathode infection (72 versus 4 hpi), Xcc massively reshaped its transcriptome with 828 differentially expressed genes (DEGs) corresponding to 18% of Xcc CDSs (Figure 1b, Tables S1 and S2). A Gene Ontology (GO) enrichment analysis identified 18 biological processes, such as catabolism, stress response and transport, that were significantly enriched in upregulated genes (Table 2). On the other hand, 13 GO terms were enriched among downregulated genes, with a strong overrepresentation of motility and chemotaxis categories (Table 2).

2.3 | Motility and chemotaxis of Xcc are strongly repressed processes inside hydathodes

Expression of most genes coding for biosynthesis of flagella and type IV pili and chemotaxis such as *fliC* (*XC_2245*, 85-fold decrease) were strongly repressed at 72 hpi compared to 4 hpi. Motility and chemotaxis are key components of pathogenicity, especially for plant pathogens (Matilla & Krell, 2018). However, Xcc seems not to be flagellated when growing in xylem fluids and the motile Xcc cells seemed less pathogenic on cauliflower and radish (Kamoun & Kado, 1990). These observations suggest a probable fitness cost of motility during plant tissue colonization. To investigate the importance of motility in disease development, we constructed mutants in key genes for the synthesis of type IV pili (Δ*pilE* and Δ*pilA*) or flagella (Δ*fliC* and Δ*fliQ*). Single and multiple mutants were tested for in vitro motility (Figure S3a), pathogenicity (Figure S3b), and hydathode colonization (Figure 2c). Despite expected motility phenotypes in vitro (Figure S3a), none of the tested mutants affected disease symptom development or hydathode colonization (Figures S3b and 2c) as might have been expected for genes whose expression is repressed inside hydathodes. Altogether, these results suggest that motility is a process that is not needed for hydathode infection.

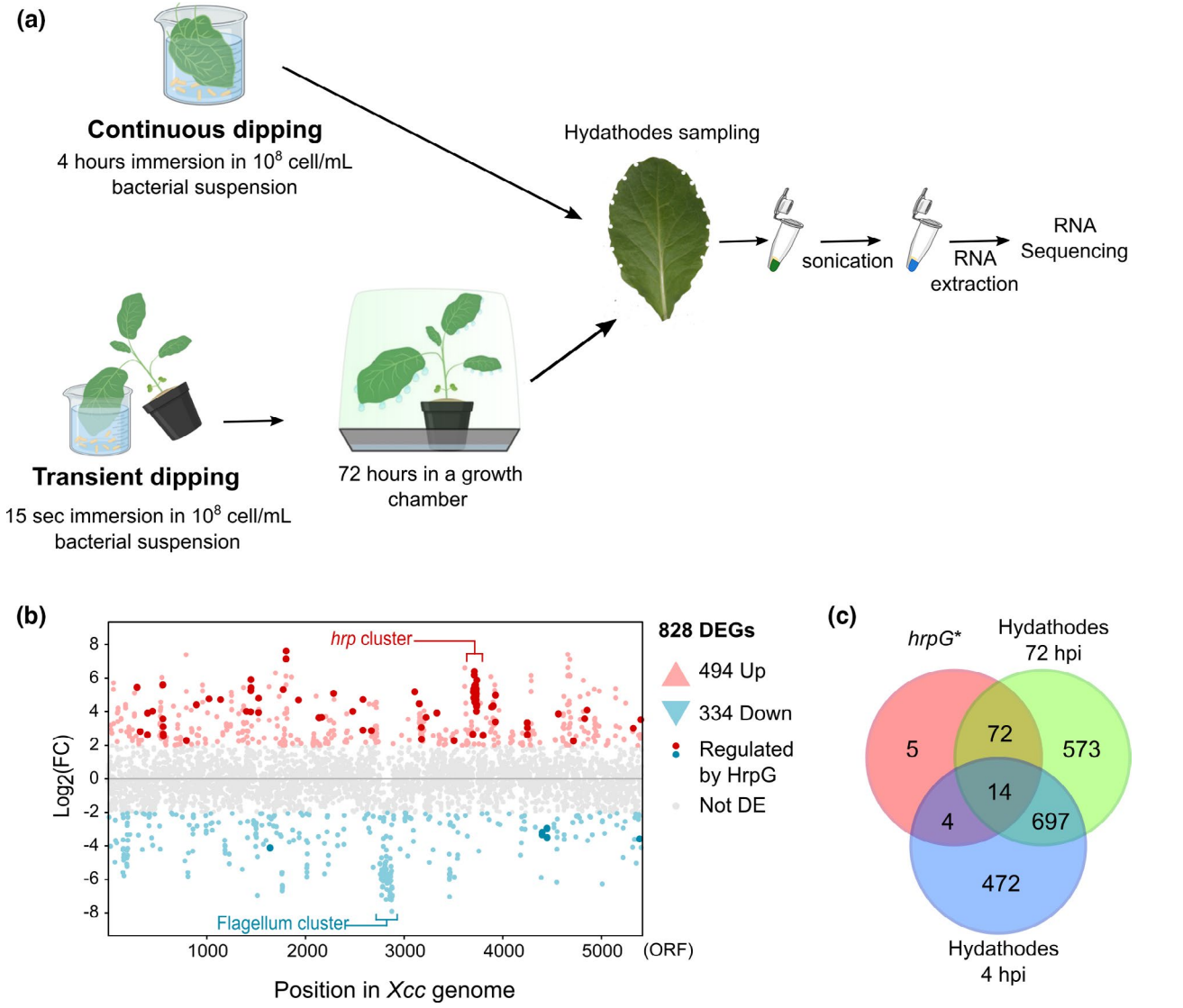

FIGURE 1 *Xanthomonas campestris* pv. *campestris* (Xcc) undergoes a massive transcriptional reprogramming during hydathode infection. (a) Schematic representation of in planta RNA sample preparation. Four-week-old cauliflower leaves were dip inoculated in a bacterial suspension for either 4 hr (upper panel) or 15 s followed by 72 hr incubation (lower panel) before hydathodes are sampled. At least 1,000 hydathodes are collected per replicate and sonicated in an RNA protect solution. RNAs were extracted from the supernatant before RNA sequencing. (b) Genomewide expression profile of Xcc in hydathodes at 72 hr postinoculation (hpi) versus 4 hpi. Each point represents a gene for which the change in expression level is given as the $\log_2$ fold change between 72 and 4 hpi into hydathodes. Differentially expressed genes (DEGs) are represented in red if induced or in blue if repressed between the two time points. Nondifferentially expressed genes are in grey. Genes under the control of the HrpG regulator (i.e., found differentially expressed in the 8004::*hrpG** vs. 8004) and found differentially expressed at 72 vs. 4 hpi in hydathodes are coloured in dark red (upregulated) and dark blue (downregulated). (c) Venn diagram showing the total number of DEGs ($|\log_2 FC| > 2$, FDR < 0.05) obtained after growth of the Xcc 8004 wildtype (WT) strain in MOKA-rich medium as compared to either the 8004::*hrpG** mutant in MOKA (in red), the WT strain after 4 hr into hydathodes (in blue) or the WT strain after 72 hr into hydathodes (in green)

2.4 | Activation of the HrpG regulon at an early stage of hydathode infection

HrpG is a known master regulator required for the expression of the T3S machinery, T3E proteins, and additional genes including plant cell wall-degrading enzymes (PCWDEs) in *Xanthomonas* spp. (Noël et al., 2001; Roux et al., 2015). In Xcc, expression of *hrpG* and 49 (out of 55) genes coding for the T3S system and type III-secreted proteins was induced at 72 hpi, suggesting the involvement of HrpG at this stage of infection (Tables S1 and S3-3). We thus investigated the biological importance of *hrpG* during hydathode infection and studied its regulon.

The 8004 Δ*hrpG* mutant showed a 10-fold reduced multiplication in hydathodes at 72 hpi (Figure 2a) and was avirulent on cauliflower after wound inoculation (Figure S3b). Both phenotypes could be complemented (Figures 2a and S3b). These results are expected

TABLE 2 GO terms of biological processes enriched among *Xanthomonas campestris* pv.*campestris* genes differentially expressed in hydathodes (72 vs. 4 hr postinoculation)

GO.ID	Term	Annotated[a]	Significant[b]	Expected[c]	Adjusted *p* values
Upregulated					
GO:0006073	Cellular glucan metabolic process	19	11	1.89	1.8×10^{-8}
GO:0055114	Oxidation-reduction process	399	74	39.78	8.9×10^{-8}
GO:0070814	Hydrogen sulphide biosynthetic process	5	5	0.5	9.5×10^{-6}
GO:0005992[e]	**Trehalose biosynthetic process**[d]	**5**	**5**	**0.5**	$\mathbf{9.5 \times 10^{-6}}$
GO:0006950	Response to stress	123	25	12.26	0.00063
GO:0019344	Cysteine biosynthetic process	6	4	0.6	0.00123
GO:0009251	Glucan catabolic process	11	5	1.1	0.00263
GO:0043649	Dicarboxylic acid catabolic process	7	4	0.7	0.00265
GO:0044247	Cellular polysaccharide catabolic process	8	4	0.8	0.00361
GO:0009306	Protein secretion	46	11	4.59	0.00435
GO:0043623	Cellular protein complex assembly	18	6	1.79	0.00612
GO:0006457	Protein folding	18	6	1.79	0.00612
GO:0098661	Inorganic anion transmembrane transport	15	5	1.5	0.01230
GO:0098869	Cellular oxidant detoxification	30	7	2.99	0.02468
GO:0044419	Interspecies interaction between organisms	12	4	1.2	0.02506
GO:0005975	Carbohydrate metabolic process	201	39	20.04	0.03559
GO:0006817	Phosphate ion transport	8	3	0.8	0.03753
GO:0016311	Dephosphorylation	33	7	3.29	0.04006
Downregulated					
GO:0006935	Chemotaxis	44	36	3.12	$<10^{-30}$
GO:0097588	**Archaeal or bacterial-type flagellum-dependent cell motility**	**23**	**23**	**1.63**	$\mathbf{9.4 \times 10^{-28}}$
GO:0007165	Signal transduction	175	51	12.4	1.7×10^{-22}
GO:0044781	**Bacterial-type flagellum organization**	**16**	**16**	**1.13**	$\mathbf{2.2 \times 10^{-19}}$
GO:0030031	Cell projection assembly	16	13	1.13	3.5×10^{-13}
GO:0000160	Phosphorelay signal transduction system	133	23	9.43	3.5×10^{-5}
GO:0000272	Polysaccharide catabolic process	27	7	1.91	0.0021
GO:0007155	Cell adhesion	5	3	0.35	0.0031
GO:0048870	**Cell motility**	**25**	**25**	**1.77**	**0.0039**
GO:0071554	Cell wall organization or biogenesis	40	6	2.83	0.0149
GO:0006468	Protein phosphorylation	79	11	5.6	0.0215
GO:0015031	Protein transport	81	12	5.74	0.0295
GO:0000302	Response to reactive oxygen species	11	3	0.78	0.0378

[a]Number of genes annotated for a given GO term.
[b]Number of differentially regulated genes among the genes annotated for a given GO term.
[c]Expected number of differentially regulated genes if no significant enrichment.
[d]Terms for which all annotated genes are differentially regulated are highlighted in bold.

because this mutant no longer expresses the T3SS, an essential virulence factor for Xcc.

To study the HrpG regulon independently of Xcc growth conditions, we decided to take advantage of a point mutation known to mimic HrpG phosphorylation, yielding a constitutively active form of HrpG named HrpG* (Wengelnik et al., 1999). This *hrpG** (E44K) gain-of-function mutation conferring constitutive expression of the HrpG regulon in vitro did not affect the multiplication of Xcc in cauliflower hydathodes (Figure 2a) nor its pathogenicity after wound inoculation relative to the wildtype strain or EPS production (Figure S3b,c). These results suggest that the gain-of-function mutation carried by HrpG* and overexpression of T3SS (see below) do not affect virulence under the inoculation protocol used.

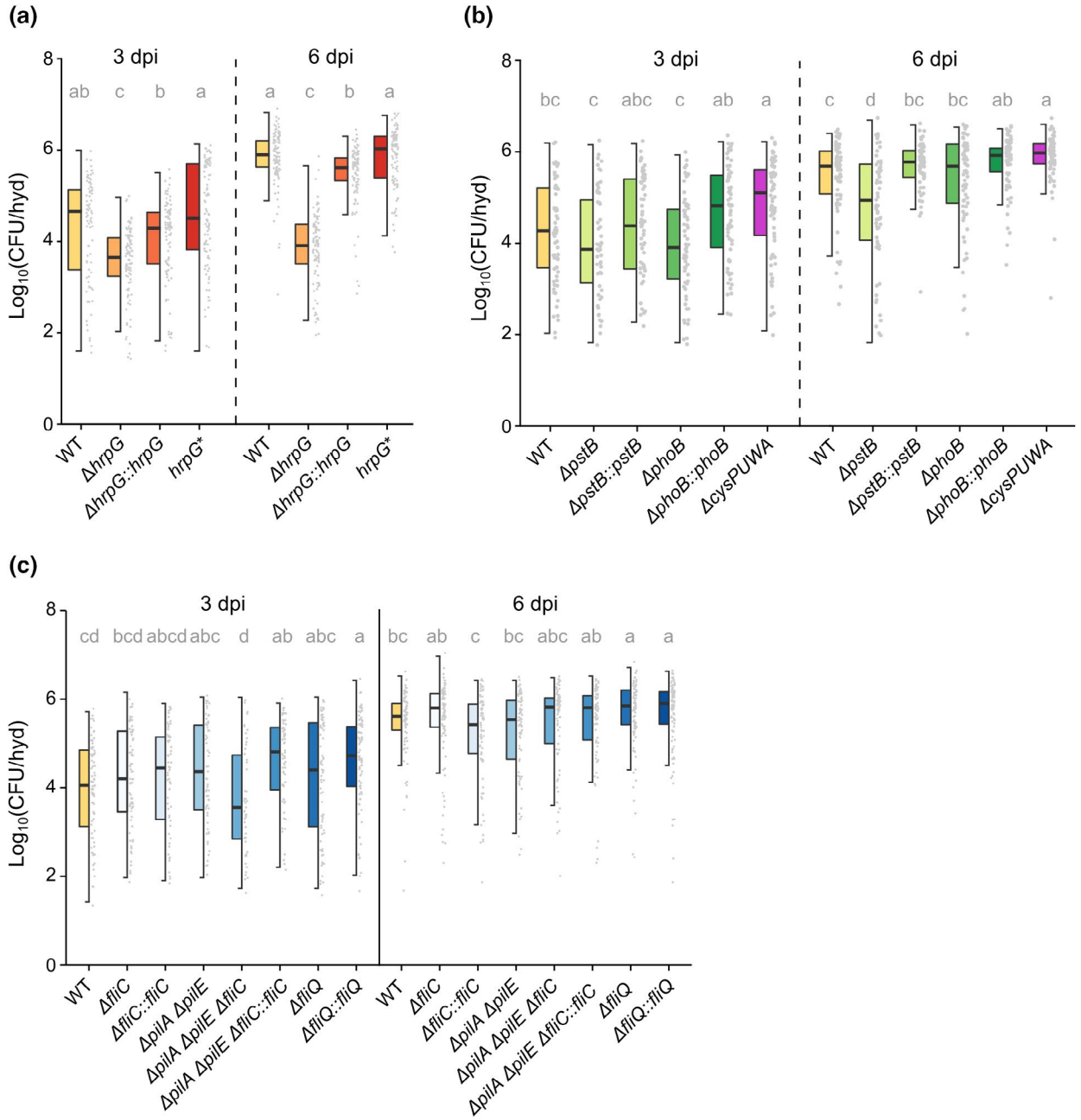

FIGURE 2 *Xanthomonas* colonization of hydathodes. Bacterial multiplication of *Xanthomonas campestris* pv. *campestris* (Xcc) 8004 wildtype strain (WT), deletion mutants, and complemented strains in individual hydathodes 3 and 6 days after dip-inoculation (dpi) of the second true leaf of 4-week-old cauliflower plants. The box plot representations show the impact of mutations (a) in the T3SS *hrpG* regulator, (b) in the phosphate and sulphate transport genes, and (c) in the motility genes over Xcc multiplication into hydathodes. Each point of the plot represents the population extracted from one hydathode. At least eight hydathodes were sampled on one leaf per plant and three plants were used per experiment, though not all hydathodes were infected. Results from at least three independent experiments were pooled and a total of at least 50 infected hydathodes were counted for each strain. Letters indicate statistically different groups obtained from the Kruskal–Wallis test on all data points for each strain with an error of $\alpha = 0.05$

To determine the extent of the HrpG regulon, we compared the transcriptomes of the 8004::*hrpG** and wildtype strains grown in MOKA medium (Tables S1 and S2). Wildtype strain 8004 does not express *hrp* genes in MOKA in contrast to strain 8004::*hrpG**. Analysis of the HrpG regulon identified 95 DEGs ($\log_2$(fold change) ≥2 or ≤−2, false discovery rate (FDR) adjusted *p* value <0.05) (Table S1). Among the 85 genes with an increased expression in strain 8004::*hrpG**, 43 possess a plant-inducible promoter box (PIP box) and are thus probably under *hrpX* control (Table S1). Thirty-nine of the 95 DEGs correspond to genes involved in T3SS and T3Es (in red and blue in Table S1, respectively) explaining the enrichment in the GO term "secretion" (GO:0,046,903) among genes upregulated in strain 8004::*hrpG** (Table 3). Expression of only 18 out of the 30 genes encoding type III secreted proteins was increased in strain 8004::*hrpG** compared

TABLE 3 GO terms of biological processes enriched among *Xanthomonas campestris* pv.*campestris* genes belonging to the HrpG regulon

GO.ID	Term	Annotated[a]	Significant[b]	Expected[c]	Adjusted *p* values
BIOLOGICAL PROCESS					
Upregulated					
GO:0002790	Peptide secretion	46	9	0.91	1.5×10^{-7}
GO:0009306	Protein secretion	46	9	0.91	1.5×10^{-7}
GO:0032940	Secretion by cell	47	9	0.93	1.8×10^{-7}
GO:0046903	Secretion	47	9	0.93	1.8×10^{-7}
GO:0015031	Protein transport	81	10	1.61	2.5×10^{-6}
GO:0008104	Protein localization	85	10	1.69	3.9×10^{-6}
GO:0015833	Peptide transport	85	10	1.69	3.9×10^{-6}
GO:0045184	Establishment of protein localization	85	10	1.69	3.9×10^{-6}
GO:0042886	Amide transport	86	10	1.71	4.3×10^{-6}
GO:0033036	Macromolecule localization	96	10	1.91	1.2×10^{-5}
GO:0071705	Nitrogen compound transport	120	10	2.38	8.6×10^{-5}
GO:0071702	Organic substance transport	142	10	2.82	0.00035
GO:0044419	Interspecies interaction between organisms	12	3	0.24	0.00143
GO:0051704	Multiorganism process	21	3	0.42	0.00763
Downregulated					
GO:0000272	Polysaccharide catabolic process	27	3	0.08	5.6×10^{-5}
GO:0009057	Macromolecule catabolic process	58	3	0.18	0.00057
GO:0016052	Carbohydrate catabolic process	61	3	0.19	0.00066
GO:0005976	Polysaccharide metabolic process	64	3	0.2	0.00076
GO:0005975	Carbohydrate metabolic process	201	4	0.63	0.00198
MOLECULAR FUNCTION					
Upregulated					
GO:0016301	Kinase activity	176	8	2.71	0.0046
GO:0001067	Regulatory region nucleic acid binding	27	3	0.42	0.0077
GO:0044212	Transcription regulatory region DNA binding	27	3	0.42	0.0077
GO:0016798	Hydrolase activity, acting on glycosyl bonds	83	5	1.28	0.0081
Downregulated					
GO:0004175	Endopeptidase activity	57	3	0.17	0.00045
GO:0004252	Serine-type endopeptidase activity	30	2	0.09	0.00315
GO:0070011	Peptidase activity, acting on L-amino acid peptides	128	3	0.38	0.00477
GO:0008233	Peptidase activity	152	3	0.45	0.00774
GO:0016829	Lyase activity	158	3	0.46	0.00863
GO:0008236	Serine-type peptidase activity	53	2	0.16	0.00964
GO:0017171	Serine hydrolase activity	53	2	0.16	0.00964

[a]Number of genes annotated for a given GO term.
[b]Number of differentially regulated genes among the genes annotated for a given GO term.
[c]Expected number of differentially regulated genes if no significant enrichment.

to 24 genes at 72 hpi inside hydathodes (Table S3-3 and Figure S2c). Among the other 56 DEGs of the HrpG regulon, 26 encode proteins with unknown function and 19 PCWDEs. Altogether, these results illustrate that the HrpG regulon is not limited to the T3SS and T3Es, and that a part of Xcc's effectome expression regulation could rely on a HrpG/HrpX-independent pathway in planta.

The HrpG regulon was almost entirely included in the in planta transcriptome (90 out of 95 genes), indicating that HrpG is activated during hydathode infection (Figures 1b,c and S2b). Eighteen genes of the HrpG regulon were overexpressed at 4 hpi in comparison to the MOKA condition, indicating that expression of the T3S machinery is initiated early during infection

(Table S1). However, the HrpG regulon (95 genes) remains a small part of Xcc transcriptomic adaptations to in planta conditions (828 genes).

2.5 | Metabolic adaptations of Xcc inside hydathodes highlight several nutritional properties of the plant environment

Among the 31 GO terms differentially enriched at the transcriptomic level, a third are involved in metabolism, indicating that Xcc undergoes an important metabolic adaptation inside the hydathode.

2.5.1 | Modification of the expression profile of genes encoding PCWDEs

We observed an increased transcription of genes involved in the catabolism of cellulose, a major component of the primary cell wall, yet there was no increased expression of other PCWDE genes, nor of *xps* and *xcs* genes encoding type II secretion systems, at 72 hpi. Among the 43 genes encoding PCWDEs in Xcc strain 8004 (da Silva et al., 2002), 10 had an increased and 10 had a reduced expression at 72 hpi (Table S3-2). These observations are consistent with the absence of visible degradation of cell walls in the epithem and suggestive of a biotrophic lifestyle (Cerutti et al., 2017).

Lignin is another major component of plant cell walls and a source of aromatic compounds. Interestingly, the expression of *XC_3426* and *XC_3427* genes coding for protocatechuate (PCA) 4;5-dioxygenase subunits was increased 6- and 8-fold at 72 hpi, respectively. PCA is a lignin degradation product (Brown et al., 2004) that can be further catabolized by PCA dioxygenases to enter the tricarboxylic acid (TCA) cycle (Wang et al., 2015). While *XC_3426* and *XC_3427* relevance for pathogenicity remains unknown, *XC_0375* to *XC_0383* genes cluster encoding 3- and 4-hydroxybenzoate degrading enzymes are needed for full virulence of Xcc in radish (Wang et al., 2015), suggesting that degradation of plant phenolic compounds happens and matters inside plant tissues.

2.5.2 | Expression of transporter genes is remodelled in planta

Broad expression changes can be observed in transporter genes as 49 out of 210 genes involved in transport were differentially expressed at 72 hpi (Tables 2 and S3-1). Those transporters belong to the major facilitator superfamily (MFS), ATP binding cassette (ABC), and TonB-dependent transporter (TBDT) families. TBDTs have been shown to be involved in iron and carbohydrate polymer uptake with high affinity in Xcc (Blanvillain et al., 2007; Boulanger et al., 2010; Dejean et al., 2013). Fourteen out of 72 TBDT genes were differentially expressed: seven showed an increased expression at 72 hpi while seven were repressed. While most have no known function, those for which expression is induced by polygalacturonate (PGA) were less expressed at 72 hpi (Table S3-1) (Blanvillain et al., 2007). The expression of two TBDT genes, *XC_3205* and *XC_2512*, which are both known to be positively regulated by HrpG and HrpX (Blanvillain et al., 2007), was induced at 72 hpi.

Interestingly, the absence of the *fur* regulon and its iron high affinity TBDT transporters (*XC_0167*, *XC_3463*, *XC_2846*, *XC_1341*, *XC_1108*, *XC_0924-0925*, *XC_0642*, *XC_4249*, *XC_0558*, and *XC_4249*) in our data set suggests that iron might not be limiting at this stage of hydathode infection.

2.5.3 | Upregulation of two pathways important for sulphur assimilation in hydathodes

In contrast to iron, induction of genes important for sulphur transport and assimilation was observed at 72 hpi in hydathodes, that is, the operon encoding the ABC sulphate transporter CysPUWA (*XC_3292* to *XC_3295*) and the operon encoding an assimilatory sulphate reduction pathway leading to sulphide production (*XC_0990* to *XC_0994*) were induced by 6- and 20-fold, respectively (Table S1). Sulphide is then available for cysteine and methionine biosynthesis. Sulphur metabolism including sulphur-containing amino acids, sulphur compounds, or sulphate has been shown to be involved in production of different virulence factors, as in xanthan production (Garcia-Ochoa et al., 2000) or T3SS induction (Schulte & Bonas, 1992). Yet, a deletion of the entire *cysPUWA* operon (Δ*XC_3292-95*) in Xcc strain 8004 did not significantly affect bacterial multiplication in hydathodes after dip-inoculation or disease symptom development after wound inoculation in cauliflower (Figures 2b and S3b). Thus, sulphate import through the CysPUWA system is not limiting for bacterial growth in hydathodes or sulphur might as well be acquired through other import pathways such as the taurine import system. For example, *Escherichia coli* responds to sulphate or cysteine starvation by expressing the *ssuABCDE* and *tauABCD* operons, which are involved in the uptake of alkanesulphonate and desulphonation of the organosulphonates and, uptake and desulphonation of taurine, respectively (Eichhorn et al., 2000; van der Ploeg et al., 1999). While *ssuABCDE* is absent in Xcc strain 8004, TauABCD homologues are encoded by genes of the locus *XC_3454* to *XC_3460*. Interestingly, expression of these genes was increased at 72 hpi, suggesting a possible implication of this pathway in sulphur assimilation in planta.

2.5.4 | Phosphate uptake machinery is rate limiting for Xcc multiplication inside hydathodes

After 72 hr in hydathodes, the increased expression of the genes encoding the PstSCAB high-affinity transporter system (genes *XC_2708* to *XC_2711*, 2- to 6-fold inductions; Tables S1 and S2), involved in active inorganic phosphate (Pi) import on phosphate starvation, suggests that Pi might be limiting inside hydathodes. This system is known to be activated in various conditions in bacteria (Lamarche et al., 2008),

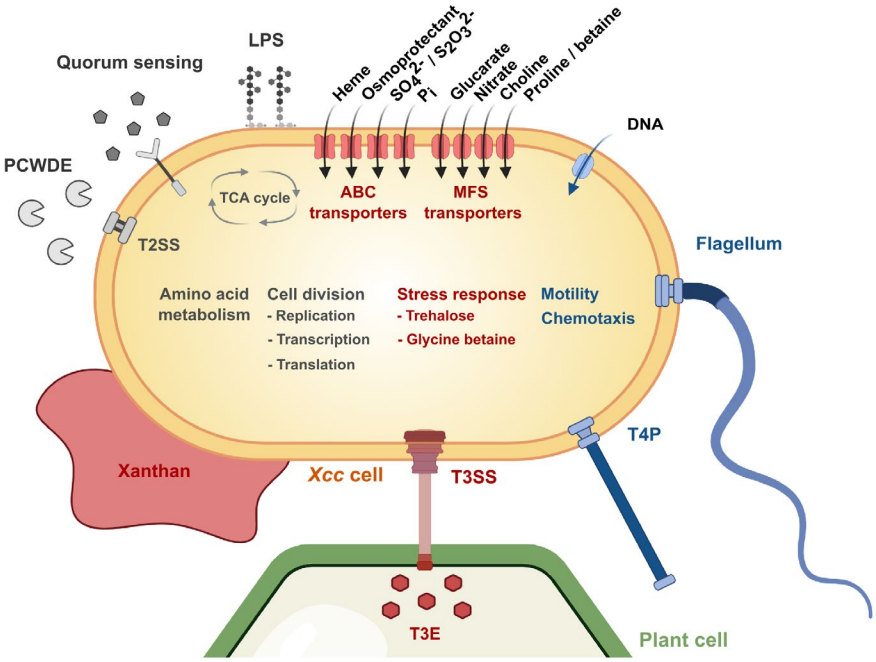

FIGURE 3 Schematic representation of main transcriptional responses of *Xanthomonas campestris* pv. *campestris* (Xcc) happening during the early stage of hydathode colonization. Genes corresponding to blue and red objects are repressed and induced between 4 and 72 hr postinoculation, respectively. Genes corresponding to grey objects are not differentially expressed. T3SS: type III secretion system; T3E: type III effector; T2SS: type II secretion system; LPS: lipopolysaccharide; PCWDE: plant cell wall-degrading enzymes; T4P: type IV pilus. Figure drafted using biorender (https://app.biorender.com)

including during plant colonization, and is essential for *Xanthomonas axonopodis* pv. *citri* (Xac) pathogenicity on citrus (Moreira et al., 2015; Pegos et al., 2014). To test if phosphate acquisition is important for Xcc strain 8004 during hydathode colonization, we mutated *XC_2711* (*pstB*) and *XC_3272*, which encode a protein homologue of the PhoB response regulator important for the *E. coli* Pi starvation response (Gardner & McCleary, 2019; Yang et al., 2012). The results obtained demonstrated that *pstB*, unlike *phoB*, is important for hydathode colonization (Figure 2b) and that both Δ*pstB* and Δ*phoB* mutants caused symptoms similar to the wildtype strain after direct inoculation into xylem vessels (Figure S3b). Observation of both increased expression of the high-affinity Pi transport system and reduced multiplication of the high-affinity phosphate transporter mutant demonstrate that Pi is limiting during hydathode infection.

Similar to Pi, expression of genes important for nitrogen assimilation such as those involved in uptake of nitrite and nitrate and their reduction to ammonia (*XC_2175* to *XC_2178*) were induced 3- to 9-fold at 72 hpi, further stressing the importance of Xcc mineral nutritional needs in hydathodes.

2.6 | Xcc adapts to nutritional, osmotic, and environmental stresses in hydathodes

Surprisingly, there were limited transcriptional changes for genes associated with transcription, translation, replication, TCA cycle, or amino acid biosynthesis between 4 and 72 hpi. However, these functions are already strongly repressed at 4 hpi compared to MOKA conditions, indicating that adaptation to the plant environment is associated with a rapid repression of cellular division and core metabolism (Tables S1 and S2). Other stress-responsive genes had an increased expression in planta such as base excision and nucleotide excision repair systems, trehalose production pathways, superoxide dismutases, and chaperone proteins. In addition, expression of the ABC transporter system *OpuB-ABC* (Hoffmann et al., 2018, XC_0173 to XC_0174) and the choline degradation pathway (Wargo, 2013, XC_0760 to XC_0761), both involved in osmoprotection, were induced at 72 hpi, suggesting that bacteria face an osmotic shock in the apoplast of the epithem cells (Table S1). Finally, expression of some genes of the *gum* operon (*XC_1658* to *XC_1673*) implicated in the production of the xanthan EPS were induced by 4- to 5-fold at 72 hpi. Xanthan is a well-known protectant against environmental stresses and toxic compounds, and prevents bacterium detection by plants (Kakkar et al., 2015). Altogether, these data seem to indicate that Xcc cells must cope with some nutritional, osmotic, and environmental stresses in hydathodes.

3 | DISCUSSION

The Xcc life cycle depends on its adaptation to various plant environments (e.g., seeds, leaf surface, hydathodes, xylem, mesophyll, debris). This work describes the transcriptional changes that Xcc undergoes on plant infection and hydathode colonization, including the regulation of various metabolic and virulence pathways (Figure 3), and informs us about the environmental conditions faced by Xcc inside hydathodes.

3.1 | Xcc adopts a sedentary biotrophic lifestyle inside hydathodes

Xcc is traditionally reported to develop necrotic lesions associated with black rot disease (Vicente & Holub, 2013). However, the

physiological snapshot obtained by RNA-Seq at 72 hpi in hydathodes suggests that Xcc first behaves as a biotroph because the epithem is intact (Cerutti et al., 2017) and many genes coding for degradative enzymes, T2SS, and most catabolic pathways of sugar polymers and carbohydrates were expressed at low levels. We also observed that the constitutive activation of the HrpG regulon recapitulating part of the in planta condition at 72 hpi was associated with reduced extracellular protease activity (Figure S3d), as observed in *Xanthomonas euvesicatoria* (Noël et al., 2001). Xcc carbon and nitrogen needs could be supported in planta by the continuous flow of xylem sap in the epithem because xylem sap contains significant concentrations of carbohydrates, amino acids, and minerals, which can be metabolized at high affinity by Xcc (Duge de Bernonville et al., 2014). Furthermore, the expression of multiple virulence-associated genes, such as those involved in quorum sensing, iron uptake, or motility, was also reduced at 72 hpi in hydathodes. Though motility has been shown to be an essential virulence trait for many bacterial pathogens (Chaban et al., 2015), Xcc motility mutants were not affected in pathogenicity as expected from genes whose expression is repressed in hydathodes. Repression of chemotaxis and motility has also been reported at early rice infection stages in *Xanthomonas oryzae* pv. *oryzicola* (Xoc) (Liao et al., 2019) while twitching motility and quorum sensing were both activated at later infection stages and are important for virulence of *Xanthomonas oryzae* pv. *oryzae* (Xoo) (Lee et al., 2017) and Xac (Li et al., 2019). Interestingly, an increase in the expression of genes important for twitching motility and adhesion was observed in Xcc grown in vitro in xylem sap (Duge de Bernonville et al., 2014). Xylem sap corresponds to the environment met by Xcc immediately after leaving the hydathode. These observations suggest a possible biphasic infectious process with the reactivation of the motility and other virulence-associated genes at later infection stages. Further transcriptomic analyses of virulence gene expression throughout the entire infection cycle would be needed to support such a hemibiotrophic lifestyle of Xcc.

3.2 | Stealthiness of Xcc inside hydathodes and neutralization of plant immune responses

The observed repression of chemotaxis, twitching, and swimming motility also suggests that those functions are dispensable if not detrimental once inside hydathodes. For instance, production of bacterial peptide flg22 from the flagellar FliC protein is a well-known pathogen-associated molecular pattern (PAMP) recognized by the FLS2 receptor and a potent elicitor of basal plant immunity (Gomez-Gomez & Boller, 2000). While $flg22_{8004}$ peptide is not recognized by *Arabidopsis* FLS2 (Guy et al., 2013a; Sun et al., 2006), we cannot exclude that other FliC peptides, flagellar proteins, or pili proteins from Xcc strain 8004 could act as PAMPs in Brassicaceae. Xcc stealthiness could also be acquired by limiting bacterial multiplication until an efficient suppression of immunity has been achieved. In contrast to a wildtype Xcc strain, a T3S system mutant unable to deliver T3E proteins inside plant cells caused hydathode browning and necrosis at 48 hpi and had a reduced multiplication at 72 hpi (Cerutti et al., 2017). These results indicate that hydathode immune responses can be effective against bacterial pathogens and that their suppression by the Xcc T3S system and its T3E proteins is required for successful infection.

3.3 | Inference of environmental conditions inside hydathodes based on Xcc transcriptomic behaviour

Xcc transcriptomic profiles can also be used to infer its metabolic and physiological status inside hydathodes and the nutritional properties of the epithem. For instance, the epithem environment is probably not limiting for assimilable iron because the corresponding uptake machinery is not expressed. In contrast, both the low-affinity phosphate inorganic transport (Pit) and the high-affinity phosphate-specific transport (Pst) systems important for the uptake of inorganic phosphate (Pi) in *Xanthomonas* are upregulated at 72 hpi (Moreira et al., 2015; Willsky & Malamy, 1980). In Xcc, we have observed that the expression of the Pst system is induced after 72 hpi in hydathodes. Although the Pst system is under the control of the PhoB response regulator, *phoB* was not differentially expressed in planta at 72 hpi in agreement with PhoB regulatory activity being dependent on its phosphorylation status rather than expression level (Gardner & McCleary, 2019). Similar to Xac (Moreira et al., 2015), the Xcc Pst system is needed for growth in planta. These results demonstrate that Xcc not only faces Pi starvation inside hydathodes but that Pi availability also limits Xcc proliferation in this tissue. Very low Pi concentrations are indeed found in the guttation fluids of several plant species, such as barley, (Nagai et al., 2013) and are correlated with expression of genes coding for plant high-affinity Pi transporters such as *AtPHT1;4* in hydathodes even under Pi-sufficient conditions (Misson et al., 2004). These observations suggest that an active competition between the plant and Xcc for access to Pi occurs in the epithem. Similar to Pi, Xcc transcriptome at 72 hpi also suggests that sulphur and nitrogen are present in low amounts, requiring the upregulation of dedicated uptake systems. Yet, it remains unclear whether these elements are limiting for growth of Xcc inside hydathodes. Exposure to stresses is also unveiled by the transcriptomic upregulation of genes involved in responses to general stress (e.g., *gum* genes) and osmotic stress. However, it remains uncertain whether osmotic stress is intrinsic of the epithemal environment or whether it is caused by plant immunity. For instance, we could not find significant evidence of oxidative stresses classically associated with strong plant immune responses. Therefore, Xcc seems to adapt rapidly to the low concentrations of nutrients found in the epithem and

to endure limited stress, maybe due to the continuous flow of fluids inside hydathodes that renews nutrient supplies and dilutes potential antibacterial compounds.

Such a global gene expression study provides a picture of the bacterial population in planta and will feed future functional genomic approaches to Xcc pathogenicity.

4 | EXPERIMENTAL PROCEDURES

4.1 | Bacterial strains, plasmids, and growth conditions

The list of strains and plasmids used in this study is provided in Table S4. Xcc was cultivated in MOKA medium (4 g/L yeast extract, 8 g/L casamino acids, 1 mM $MgSO_4$, 2 g/L K_2HPO_4) at 28 °C under agitation at 200 rpm or on MOKA-agar plates (Blanvillain et al., 2007). *E. coli* TG1 and strain-carrying pRK2073 helper plasmid were cultivated in liquid Luria Bertani (LB) medium under agitation or on LB agar plates at 37 °C. Antibiotics were used at the following concentrations: 50 μg/ml rifampicin, 50 μg/ml kanamycin, and 40 μg/ml spectinomycin.

4.2 | Mutagenesis and complementation

In-frame deletion mutants of Xcc were obtained by double recombination with derivatives of the suicide plasmid pK18mobSacB as described (Schafer et al., 1994). Sequences flanking the deletion were amplified from Xcc strain 8004 genomic DNA and introduced into pK18mobSacB by Gibson assembly (Gibson et al., 2009). For complementation, the CDS was amplified from Xcc strain 8004 genomic DNA and cloned by Gibson assembly into plasmid pK18_CompR3, a pK18mobSacB derivative containing a pTac promoter and a T7 terminator region from pCZ1016 (Dejean et al., 2013) flanked by *XC_1301* and *XC_1302* sequences to drive stable insertion at the *XC_1301/XC_1302* interval. For genes lacking a ribosome-binding site (RBS) in their upstream region, the RBS from plasmid pK18-*GUS-GFP* (Cerutti et al., 2017) was inserted downstream of the pTac promoter, giving pK18_compR3_RBS. All plasmids were conjugated into Xcc 8004::*GUS-GFP* derivatives by triparental mating with the *E. coli* TG1 carrying pRK2073 helper plasmid as described (Cerutti et al., 2017; Ditta et al., 1980; Figurski & Helinski, 1979). The sequences of oligonucleotides used to construct deletion and complementation plasmids are listed in Table S5. The growth of all strains was assessed in MME and MOKA media (Figure S4).

4.3 | Plant growth conditions

Brassica oleracea var *.botrytis* 'Clovis F1' (cauliflower) was grown under greenhouse conditions. Four-week-old plants were transferred 1 day before inoculations in a growth chamber (9 hr light, 22 °C, 70% relative humidity).

4.4 | Preparation of biological samples used for RNA-Seq

For in vitro RNA-Seq experiments, RNAs were extracted from Xcc strains grown in MOKA medium to exponential phase ($OD_{600\,nm}$ between 0.5 and 0.7), harvested by filtration as described (Roux et al., 2015), and stored at −80 °C.

For in planta RNA-Seq experiments, RNA was extracted from infected hydathodes sampled from the first three cauliflower leaves after inoculation by continuous or transient dipping in a bacterial suspension of 10^8 cfu/ml as described (Cerutti et al., 2017) using 0.01% of SILWET-L77 (DE SANGOSSE) (Figure 1a). These first three leaves of 4-week-old plants show mature hydathodes on leaf margins that can be successfully infected with Xcc. For inoculations by continuous dipping, detached leaves were dipped in the bacterial suspension for 4 hr and hydathodes were immediately harvested. For inoculations by transient dipping, leaves (attached to the plant) were dipped in a bacterial suspension for c.15 s. Plants were placed in a domed propagator, watered, and covered for a day and a half (95%–100% humidity). Hydathodes were harvested 72 hpi. To determine the level of infection of hydathodes under both continuous and transient dipping inoculation protocols, the bacterial populations were determined at 4 and 72 hpi in 24 and 30 individual hydathodes, respectively (Figure S1b), as described below. Based on those results, these two inoculation methods allow the comparison of similar bacterial populations (around 10^5 bacteria per hydathode) having spent either 4 or 72 hr inside hydathodes.

To collect hydathodes, leaves were briefly rinsed twice in sterile distilled water and dried on a paper towel prior to harvesting. At least 1,000 hydathodes were macrodissected per condition with a 1.5 mm diameter punch. Collected tissues were immediately placed in RNA Protect Bacteria Reagent (Qiagen, 2:1 [vol/vol] of RNA Protect and RNase-free water). After 3 min sonication in a water bath, the supernatant was recovered and centrifuged for 10 min at 5,000 × g. The pellet was stored at −80 °C. Three independent biological replicates were sampled.

4.5 | RNA extractions, ribodepletion, and sequencing

RNA extraction and ribodepletion were performed as previously described (Sallet et al., 2013). Oligonucleotide probes used for RNA depletion were directed against *Xanthomonas* rRNA and 2 tRNA (Ile and Ala) (Roux et al., 2015) and for plant-derived samples probes targeting *Arabidopsis* and *Brassica oleracea* rRNA and major chloroplastic RNA (Sallet et al., 2013) (Table S5). RNAs were fractionated into short (<200 nt) and long (>200 nt) RNA fractions using Zymo Research RNA Clean & Concentrator TM-5 columns (Proteigene) and subjected to oriented sequencing (see Supplementary material and methods for detailed procedures). Raw sequence data were submitted to the Sequence Read Archive (SRA) database (accessions SRP280320 and SRP280329).

TABLE 4 Properties of RNAseq libraries from *Xcc* strain 8004 wild-type and derivatives grown in vitro or harvested from cauliflower hydathodes

RNA size	Strain	Condition	Biological replicates	Number of raw reads	Uniquely mapped reads *Xcc* and *Brassica* (%)[a]	Hits *Brassica* genes (%)[b]	Hits *Xcc* genes (%)[c]	Accession[d]
Long RNAs fraction	8004	MOKA	3	22 503 680	93.58	–	9,472	SRR12603737
				31 781 601	88.67	–	9,449	SRR12603738, SRR12603725
				29 317 932	88.54	–	9,421	SRR12603739, SRR12603726
Small RNAs fraction			3	14 141 422	–	–	–	SRR12603734
				13 443 960	–	–	–	SRR12603735
				13 423 070	–	–	–	SRR12603736
Long RNAs fraction	8004::*hrpG**	MOKA	3	21 746 450	9,587	–	9,358	SRR12603727
				14 282 665	94.84	–	9,411	SRR12603728
				15 932 094	95.08	–	9,457	SRR12603729
Small RNAs fraction			4	10 314 675	–	–	–	SRR12603720
				11 898 842	–	–	–	SRR12603721
				10 794 476	–	–	–	SRR12603722
				14 113 815	–	–	–	SRR12603733
	8004	Cauliflower hydathodes 4 hpi	3	158 422 507	33.42	6,245	1,332	SRR12603813, SRR12603814, SRR12603815
				150 271 178	23.49	6,621	1,063	SRR12603810, SRR12603811, SRR12603812
				173 591 985	41.15	6,794	1,012	SRR12603804, SRR12603805, SRR12603806
	8004	Cauliflower hydathodes 72 hpi	3	164 579 058	38.59	5,519	1,640	SRR12603816, SRR12603817, SRR12603818
				163 894 181	38.47	5,256	2,727	SRR12603801, SRR12603802, SRR12603803
				143 337 188	27.63	73.48	1.61	SRR12603807. SRR12603808, SRR12603809

[a]Percentage of raw reads mapped uniquely to the sequences of *Xcc* strain 8004 chromosome (Genbank accession number CP000050.1), *Brassica oleracea* nuclear and mitochondrial genomes (Accession GCA_000695525.1, NC_016118.1), and *Brassica rapa* chloroplastic genome (BRARA_CHL, accession NC_040849.1).

[b]Percentage of unique hits to the genes of *Brassica oleracea* nuclear and mitochondrial genomes and *Brassica rapa* chloroplastic genome.

[c]Percentage of unique hits to the genes of *Xcc* strain 8004.

[d]Sequence Read Archive accession number.

4.6 | Reannotation of Xcc strain 8004 genome sequence

Annotation of *X. campestris* pv. *campestris* strain 8004 genome was performed using EuGene-PP (Sallet et al., 2013) (EuGene-PP v. 1.0, eugene-4.1c) with SRP280320 RNA libraries and *X. campestris* pv. *campestris* strains 8004, ATCC33913, and B100 public annotations GCA_000012105.1, GCA_000007145.1, and GCA_000070605.1, respectively (Qian et al 2005; Vorholter et al., 2008). This new annotation is available at https://dx.doi.org/10.25794/reference/id52ofys.

4.7 | Analysis of RNA-Seq results and statistical analysis

Mapping of RNA-Seq reads was performed on the Xcc strain 8004 reannotated genome sequence (Qian et al., 2005, Genbank accession number CP000050.1) and when appropriate on sequences of *B. oleracea* nuclear genome (Brassica_oleracea v. 2.1.31; accession GCA_000695525.1), *B. oleracea* mitochondrial genome (accession NC_016118.1), and *Brassica rapa* chloroplastic genome (BRARA_CHL, accession NC_040849.1) as described (Roux et al., 2015).

DEGs were detected with EdgeR Bioconductor package v. 3.30.3 (Robinson & Smyth, 2008). Genes with no counts across all libraries were discarded. Normalization was performed using the trimmed mean of M-values method (Robinson & Oshlack, 2010). Quality control plots of normalized data sets and reproducibility of biological repeats were generated by principal component analysis using the Ade4 v. 7-15 package (Dray & Dufour, 2007) and heatmaps obtained with the package pheatmap v. 1.0.12 (Raivo Kolde (2015). pheatmap: Pretty Heatmaps. R package v. 1.0.8. https://CRAN.R-project.org/package=pheatmap) on sample-to-sample Euclidean distances.

Fitted generalized linear models (GLMs) with a design matrix multiple factor (biological repetition and factor of interest) were designed. The Cox–Reid profile-adjusted likelihood (CR) method in estimating dispersions was used. DEGs were called using the GLM likelihood ratio test using a false discovery rate (FDR) (Benjamini & Yekutieli, 2001) adjusted p value < 0.05. Clustering on filtered DEG ($p < 0.05$ in at least one biological condition) was generated with heatmap.2 function as available in the gplots Bioconductor package v. 3.0.1. (Warnes et al., 2015) using Ward's minimum variance clustering method on Euclidean (Murtagh & Legendre, 2014). Analysis of GO enrichment was conducted using the topGO package v. 2.40.0 (Alexa et al., 2006).

4.8 | Infection of hydathodes and measurement of bacterial population

For hydathode infection, the second true leaf of cauliflower plants was dip-inoculated in a bacterial suspension at 10^8 cfu/ml in 1 mM $MgCl_2$ containing 0.5% (vol/vol) Tween 80. To determine Xcc populations in single hydathodes, hydathodes were collected at 3 or 6 dpi by macrodissection with a 1.5 mm diameter punch. Eight hydathodes were sampled per leaf and individually placed in 200 µl of 1 mM $MgCl_2$. After bead-assisted grinding at 30 Hz for 2 min using a Retsch MM400 grinder, 5 µl droplets of serial dilutions were spotted on MOKA plates supplemented with 30 µg/ml pimaricin in three technical replicates and incubated at 28 °C for 2–3 days. Individual colonies were counted and the mean of the three technical replicates was calculated to estimate the infection level of each hydathode. Experiments were performed on three plants per condition and in three independent biological replicates.

Significance of differences observed in bacterial population quantifications and bacterial pathogenicity assays were assessed using the nonparametric Kruskal–Wallis test with $\alpha = 0.05$.

ACKNOWLEDGEMENTS

A.C. and J.L. were funded by a PhD grant from the French Ministry of Higher Education, Research and Innovation. B.R., E.L., A.C., M.A., and L.D.N. were funded by grants from the Agence Nationale de la Recherche XANTHOMIX (ANR-2010-GENM-013-02), Xopaque (ANR-10-JCJC-1703-01), and NEPHRON (ANR-18-CE20-0020-01). We are grateful to Stéphanie Bolot for management and early analysis of the Xanthomix data set. J.L., E.L., A.B., R.B., M.A., and L.D.N. were funded by the XBOX (ANR-19-CE20-JCJC-0014-01) project. The Laboratoire des Interactions Plantes-Microbes-Environnement is part of the French Laboratory of Excellence project (TULIP ANR-10-LABX-41; ANR-11-IDEX-0002-02). All authors benefited from the COST action CA16107 EuroXanth.

CONFLICT OF INTEREST

The authors declare no conflict of interest.

OPEN RESEARCH BADGES

This article has earned an Open Data badge for making publicly available the digitally-shareable data necessary to reproduce the reported results. The data is available at https://dx.doi.org/10.25794/reference/id52ofys.

DATA AVAILABILITY STATEMENT

Genome annotation accession numbers and sequence read archive accession numbers for RNA-Seq libraries are openly available as indexed in Tables 1 and 4, respectively.

ORCID

Julien S. Luneau https://orcid.org/0000-0002-1917-3468
Alice Boulanger https://orcid.org/0000-0001-5918-9547
Laurent D. Noël https://orcid.org/0000-0002-0110-1423

REFERENCES

Alexa, A., Rahnenfuhrer, J. & Lengauer, T. (2006) Improved scoring of functional groups from gene expression data by decorrelating GO graph structure. *Bioinformatics*, 22, 1600–1607.

Alkhateeb, R.S., Vorhölter, F.-J., Rückert, C., Mentz, A., Wibberg, D., Hublik, G. et al. (2016) Genome wide transcription start sites analysis

of *Xanthomonas campestris* pv. *campestris* B100 with insights into the gum gene cluster directing the biosynthesis of the exopolysaccharide xanthan. *Journal of Biotechnology*, 225, 18–28.

An, S.Q., Allan, J.H., McCarthy, Y., Febrer, M., Dow, J.M. & Ryan, R.P. (2014) The PAS domain-containing histidine kinase RpfS is a second sensor for the diffusible signal factor of *Xanthomonas campestris*. *Molecular Microbiology*, 92, 586–597.

Benjamini, Y. & Yekutieli, D. (2001) The control of the false discovery rate in multiple testing under dependency. *Annals of Statistics*, 29, 1165–1188.

Blanvillain, S., Meyer, D., Boulanger, A., Lautier, M., Guynet, C., Denancé, N. et al. (2007) Plant carbohydrate scavenging through TonB-dependent receptors: a feature shared by phytopathogenic and aquatic bacteria. *PLoS One*, 2, e224.

Boulanger, A., Dejean, G., Lautier, M., Glories, M., Zischek, C., Arlat, M. et al. (2010) Identification and regulation of the N-acetylglucosamine utilization pathway of the plant pathogenic bacterium *Xanthomonas campestris* pv. *campestris*. *Journal of Bacteriology*, 192, 1487–1497.

Brown, C.K., Vetting, M.W., Earhart, C.A. & Ohlendorf, D.H. (2004) Biophysical analyses of designed and selected mutants of protocatechuate 3,4-dioxygenase1. *Annual Review of Microbiology*, 58, 555–585.

Buttner, D. & Bonas, U. (2010) Regulation and secretion of *Xanthomonas* virulence factors. *FEMS Microbiology Reviews*, 34, 107–133.

Carlton, W.M., Braun, E.J. & Gleason, M.L. (1998) Ingress of *Clavibacter michiganensis* subsp. *michiganensis* into tomato leaves through hydathodes. *Phytopathology*, 88, 525–529.

Cerutti, A., Jauneau, A., Auriac, M.-C., Lauber, E., Martinez, Y., Chiarenza, S. et al. (2017) Immunity at cauliflower hydathodes controls systemic infection by *Xanthomonas campestris* pv. *campestris*. *Plant Physiology*, 174, 700–716.

Cerutti, A., Jauneau, A., Laufs, P., Leonhardt, N., Schattat, M.H., Berthomé, R. et al. (2019) Mangroves in the leaves: anatomy, physiology, and immunity of epithemal hydathodes. *Annual Review of Phytopathology*, 57, 91–116.

Chaban, B., Hughes, H.V. & Beeby, M. (2015) The flagellum in bacterial pathogens: For motility and a whole lot more. *Seminars in Cell & Developmental Biology*, 46, 91–103.

Chen, X., Sun, C., Laborda, P., Zhao, Y., Palmer, I., Fu, Z.Q. et al. (2018) Melatonin treatment inhibits the growth of *Xanthomonas oryzae* pv. *oryzae*. *Frontiers in Microbiology*, 9, 2280.

Daniels, M.J., Barber, C.E., Turner, P.C., Sawczyc, M.K., Byrde, R.J. & Fielding, A.H. (1984) Cloning of genes involved in pathogenicity of *Xanthomonas campestris* pv. *campestris* using the broad host range cosmid pLAFR1. *The EMBO Journal*, 3, 3323–3328.

Darsonval, A., Darrasse, A., Durand, K., Bureau, C., Cesbron, S. & Jacques, M.A. (2009) Adhesion and fitness in the bean phyllosphere and transmission to seed of *Xanthomonas fuscans* subsp. *fuscans*. *Molecular Plant-Microbe Interactions*, 22, 747–757.

Dejean, G., Blanvillain-Baufume, S., Boulanger, A., Darrasse, A., Duge de Bernonville, T., Girard, A.L. et al. (2013) The xylan utilization system of the plant pathogen *Xanthomonas campestris* pv. *Campestris* controls epiphytic life and reveals common features with oligotrophic bacteria and animal gut symbionts. *New Phytologist*, 198, 899–915.

Ditta, G., Stanfield, S., Corbin, D. & Helinski, D.R. (1980) Broad host range DNA cloning system for Gram-negative bacteria: Construction of a gene bank of *Rhizobium meliloti*. *Proceedings of the National Academy of Sciences of the United States of America*, 77, 7347–7351.

Dray, S. & Dufour, A.-B. (2007) The Ade4 package: implementing the duality diagram for ecologists. *Journal of Statistical Software*, 22, 1–20.

Duge de Bernonville, T., Noël, L.D., Sancristobal, M., Danoun, S., Becker, A., Soreau, P. et al. (2014) Transcriptional reprogramming and phenotypical changes associated with growth of *Xanthomonas campestris* pv. *campestris* in cabbage xylem sap. *FEMS Microbiology Ecology*, 89, 527–541.

Dutta, B., Gitaitis, R., Sanders, H., Booth, C., Smith, S., Langston, D.B. et al. (2014) Role of blossom colonization in pepper seed infestation by *Xanthomonas euvesicatoria*. *Phytopathology*, 104, 232–239.

Eichhorn, E., van der Ploeg, J.R. & Leisinger, T. (2000) Deletion analysis of the *Escherichia coli* taurine and alkanesulfonate transport systems. *Journal of Bacteriology*, 182, 2687–2695.

Figurski, D.H. & Helinski, D.R. (1979) Replication of an origin-containing derivative of plasmid RK2 dependent on a plasmid function provided *in trans*. *Proceedings of the National Academy of Sciences of the United States of America*, 76, 1648–1652.

Fukui, R., Fukui, H., McElhaney, R., Nelson, S.C. & Alvarez, A.M. (1996) Relationship between symptom development and actual sites of infection in leaves of *Anthurium* inoculated with a bioluminescent strain of *Xanthomonas campestris* pv. *dieffenbachiae*. *Applied and Environmental Microbiology*, 62, 1021–1028.

Garcia-Ochoa, F., Santos, V.E., Casas, J.A. & Gomez, E. (2000) Xanthan gum: production, recovery, and properties. *Biotechnology Advances*, 18, 549–579.

Gardner, S.G. & McCleary, W.R. (2019) Control of the *phoBR* Regulon in *Escherichia coli*. *EcoSal Plus*, 8. https://doi.org/10.1128/ecosalplus.ESP-0006-2019

Getaz, M., Pulawska, J., Smits, T.H.M. & Pothier, J.F. (2020) Host–pathogen interactions between *Xanthomonas fragariae* and its host *Fragaria* × *ananassa* investigated with a dual RNA-Seq analysis. *Microorganisms*, 8, 1253.

Gibson, D.G., Young, L., Chuang, R.Y., Venter, J.C., Hutchison, C.A. 3RD & Smith, H.O. (2009) Enzymatic assembly of DNA molecules up to several hundred kilobases. *Nature Methods*, 6, 343–345.

Gomez-Gomez, L. & Boller, T. (2000) FLS2: an LRR receptor-like kinase involved in the perception of the bacterial elicitor flagellin in *Arabidopsis*. *Molecular Cell*, 5, 1003–1011.

Guy, E., Genissel, A., Hajri, A., Chabannes, M., David, P., Carrère, S. et al. (2013a) Natural genetic variation of *Xanthomonas campestris* pv. *campestris* pathogenicity on *Arabidopsis* revealed by association and reverse genetics. *mBio*, 4, e00538-12.

Guy, E., Lautier, M., Chabannes, M., Roux, B., Lauber, E., Arlat, M. et al. (2013b) *xopAC*-triggered immunity against *Xanthomonas* depends on *Arabidopsis* receptor-like cytoplasmic kinase genes *PBL2* and *RIPK*. *PLoS One*, 8, e73469.

He, Y.W. & Zhang, L.H. (2008) Quorum sensing and virulence regulation in *Xanthomonas campestris*. *FEMS Microbiology Reviews*, 32, 842–857.

Hoffmann, T., Warmbold, B., Smits, S.H.J., Tschapek, B., Ronzheimer, S., Bashir, A. et al. (2018) Arsenobetaine: an ecophysiologically important organoarsenical confers cytoprotection against osmotic stress and growth temperature extremes. *Environmental Microbiology*, 20, 305–323.

Hugouvieux, V., Barber, C.E. & Daniels, M.J. (1998) Entry of *Xanthomonas campestris* pv. *campestris* into hydathodes of *Arabidopsis thaliana* leaves: a system for studying early infection events in bacterial pathogenesis. *Molecular Plant-Microbe Interactions*, 11, 537–543.

Jalan, N., Kumar, D., Andrade, M.O., Yu, F., Jones, J.B., Graham, J.H. et al. (2013) Comparative genomic and transcriptome analyses of pathotypes of *Xanthomonas citri* subsp. *citri* provide insights into mechanisms of bacterial virulence and host range. *BMC Genomics*, 14, 551.

Kakkar, A., Nizampatnam, N.R., Kondreddy, A., Pradhan, B.B. & Chatterjee, S. (2015) *Xanthomonas campestris* cell-cell signalling molecule DSF (diffusible signal factor) elicits innate immunity in plants and is suppressed by the exopolysaccharide xanthan. *Journal of Experimental Botany*, 66, 6697–6714.

Kamoun, S. & Kado, C.I. (1990) Phenotypic switching affecting chemotaxis, xanthan production, and virulence in *Xanthomonas campestris*. *Applied and Environmental Microbiology*, 56, 3855–3860.

Kim, S., Cho, Y.J., Song, E.S., Lee, S.H., Kim, J.G. & Kang, L.W. (2016) Time-resolved pathogenic gene expression analysis of the plant pathogen *Xanthomonas oryzae* pv. *oryzae*. *BMC Genomics*, 17, 345.

Lamarche, M.G., Wanner, B.L., Crepin, S. & Harel, J. (2008) The phosphate regulon and bacterial virulence: a regulatory network connecting phosphate homeostasis and pathogenesis. *FEMS Microbiology Reviews*, 32, 461–473.

Lee, S.E., Gupta, R., Jayaramaiah, R.H., Lee, S.H., Wang, Y., Park, S.R. et al. (2017) Global transcriptome profiling of *Xanthomonas oryzae* pv. *oryzae* under in planta growth and in vitro culture conditions. *The Plant Pathology Journal*, 33, 458–466.

Li, L., Li, J., Zhang, Y. & Wang, N. (2019) Diffusible signal factor (DSF)-mediated quorum sensing modulates expression of diverse traits in *Xanthomonas citri* and responses of citrus plants to promote disease. *BMC Genomics*, 20, 55.

Liao, C.-T., Liu, Y.-F., Chiang, Y.-C., Lo, H.-H., Du, S.-C., Hsu, P.-C. et al. (2016) Functional characterization and transcriptome analysis reveal multiple roles for Prc in the pathogenicity of the black rot pathogen *Xanthomonas campestris* pv. *campestris*. *Research in Microbiology*, 167, 299–312.

Liao, Z.X., Ni, Z., Wei, X.L., Chen, L., Li, J.Y., Yu, Y.H. et al. (2019) Dual RNA-seq of *Xanthomonas oryzae* pv. *oryzicola* infecting rice reveals novel insights into bacterial-plant interaction. *PLoS One*, 14, e0215039.

Liu, W., Yu, Y.H., Cao, S.Y., Niu, X.N., Jiang, W., Liu, G.F. et al. (2013) Transcriptome profiling of *Xanthomonas campestris* pv. *campestris* grown in minimal medium MMX and rich medium NYG. *Research in Microbiology*, 164, 466–479.

Matilla, M.A. & Krell, T. (2018) The effect of bacterial chemotaxis on host infection and pathogenicity. *FEMS Microbiology Reviews*, 42, fux052.

Misson, J., Thibaud, M.C., Bechtold, N., Raghothama, K. & Nussaume, L. (2004) Transcriptional regulation and functional properties of *Arabidopsis* Pht1;4, a high affinity transporter contributing greatly to phosphate uptake in phosphate deprived plants. *Plant Molecular Biology*, 55, 727–741.

Moreira, L.M., Facincani, A.P., Ferreira, C.B., Ferreira, R.M., Ferro, M.I., Gozzo, F.C. et al. (2015) Chemotactic signal transduction and phosphate metabolism as adaptive strategies during citrus canker induction by *Xanthomonas citri*. *Functional & Integrative Genomics*, 15, 197–210.

Murtagh, F. & Legendre, P. (2014) Ward's hierarchical agglomerative clustering method: which algorithms implement Ward's criterion? *Journal of Classification*, 31, 274–295.

Nagai, M., Ohnishi, M., Uehara, T., Yamagami, M., Miura, E., Kamakura, M. et al. (2013) Ion gradients in xylem exudate and guttation fluid related to tissue ion levels along primary leaves of barley. *Plant, Cell and Environment*, 36, 1826–1837.

Nino-Liu, D.O., Ronald, P.C. & Bogdanove, A.J. (2006) *Xanthomonas oryzae* pathovars: model pathogens of a model crop. *Molecular Plant Pathology*, 7, 303–324.

Nobori, T., Velasquez, A.C., Wu, J., Kvitko, B.H., Kremer, J.M., Wang, Y. et al. (2018) Transcriptome landscape of a bacterial pathogen under plant immunity. *Proceedings of the National Academy of Sciences of the United States of America*, 115, E3055–E3064.

Noël, L., Thieme, F., Nennstiel, D. & Bonas, U. (2001) cDNA-AFLP analysis unravels a genome-wide *hrpG*-regulon in the plant pathogen *Xanthomonas campestris* pv. *vesicatoria*. *Molecular Microbiology*, 41, 1271–1281.

Noh, T.H., Song, E.S., Kim, H.I., Kang, M.H. & Park, Y.J. (2016) Transcriptome-based identification of differently expressed genes from *Xanthomonas oryzae* pv. *oryzae* strains exhibiting different virulence in rice varieties. *International Journal of Molecular Sciences*, 17, 259.

Pegos, V.R., Nascimento, J.F., Sobreira, T.J., Pauletti, B.A., Paes-Leme, A. & Balan, A. (2014) Phosphate regulated proteins of *Xanthomonas citri* subsp. *citri*: a proteomic approach. *Journal of Proteomics*, 108, 78–88.

Qian, W., Han, Z.J. & He, C. (2008) Two-component signal transduction systems of *Xanthomonas* spp.: a lesson from genomics. *Molecular Plant-Microbe Interactions*, 21, 151–161.

Qian, W., Jia, Y., Ren, S.X., He, Y.Q., Feng, J.X., Lu, L.F. et al. (2005) Comparative and functional genomic analyses of the pathogenicity of phytopathogen *Xanthomonas campestris* pv. *campestris*. *Genome Research*, 15, 757–767.

Robene-Soustrade, I., Laurent, P., Gagnevin, L., Jouen, E. & Pruvost, O. (2006) Specific detection of *Xanthomonas axonopodis* pv. *dieffenbachiae* in anthurium (*Anthurium andreanum*) tissues by nested PCR. *Applied and Environmental Microbiology*, 72, 1072–1078.

Robinson, M.D. & Oshlack, A. (2010) A scaling normalization method for differential expression analysis of RNA-seq data. *Genome Biology*, 11, R25.

Robinson, M.D. & Smyth, G.K. (2008) Small-sample estimation of negative binomial dispersion, with applications to SAGE data. *Biostatistics*, 9, 321–332.

Roux, B., Bolot, S., Guy, E., Denance, N., Lautier, M., Jardinaud, M.F. et al. (2015) Genomics and transcriptomics of *Xanthomonas campestris* species challenge the concept of core type III effectome. *BMC Genomics*, 16, 975.

Sallet, E., Roux, B., Sauviac, L., Jardinaud, M.-f., Carrere, S., Faraut, T. et al. (2013) Next-generation annotation of prokaryotic genomes with EuGene-P: application to *Sinorhizobium meliloti* 2011. *DNA Research*, 20, 339–354.

Schafer, A., Tauch, A., Jager, W., Kalinowski, J., Thierbach, G. & Puhler, A. (1994) Small mobilizable multi-purpose cloning vectors derived from the *Escherichia coli* plasmids pK18 and pK19: selection of defined deletions in the chromosome of *Corynebacterium glutamicum*. *Gene*, 145, 69–73.

Schmidtke, C., Findeiss, S., Sharma, C.M., Kuhfuss, J., Hoffmann, S., Vogel, J. et al. (2012) Genome-wide transcriptome analysis of the plant pathogen *Xanthomonas* identifies sRNAs with putative virulence functions. *Nucleic Acids Research*, 40, 2020–2031.

Schulte, R. & Bonas, U. (1992) A *Xanthomonas* pathogenicity locus is induced by sucrose and sulfur-containing amino acids. *The Plant Cell*, 4, 79–86.

da Silva, A.C., Ferro, J.A., Reinach, F.C., Farah, C.S., Furlan, L.R., Quaggio, R.B. et al. (2002) Comparison of the genomes of two *Xanthomonas* pathogens with differing host specificities. *Nature*, 417, 459–463.

Sun, W., Dunning, F.M., Pfund, C., Weingarten, R. & Bent, A.F. (2006) Within-species flagellin polymorphism in *Xanthomonas campestris* pv *campestris* and its impact on elicitation of *Arabidopsis FLAGELLIN SENSING2*-dependent defenses. *The Plant Cell*, 18, 764–779.

Tao, F., He, Y.W., Wu, D.H., Swarup, S. & Zhang, L.H. (2010) The cyclic nucleotide monophosphate domain of *Xanthomonas campestris* global regulator Clp defines a new class of cyclic di-GMP effectors. *Journal of Bacteriology*, 192, 1020–1029.

van der Ploeg, J.R., Iwanicka-Nowicka, R., Bykowski, T., Hryniewicz, M.M. & Leisinger, T. (1999) The *Escherichia coli ssuEADCB* gene cluster is required for the utilization of sulfur from aliphatic sulfonates and is regulated by the transcriptional activator Cbl. *Journal of Biological Chemistry*, 274, 29358–29365.

Vicente, J.G. & Holub, E.B. (2013) *Xanthomonas campestris* pv. *campestris* (cause of black rot of crucifers) in the genomic era is still a worldwide threat to brassica crops. *Molecular Plant Pathology*, 14, 2–18.

Vorhölter, F.J., Schneiker, S., Goesmann, A., Krause, L., Bekel, T., Kaiser, O., et al. (2008) The genome of *Xanthomonas campestris* pv. *campestris* B100 and its use for the reconstruction of metabolic pathways involved in xanthan biosynthesis. *Journal of Biotechnology*, 134, 33–45.

Wang, J.Y., Zhou, L., Chen, B., Sun, S., Zhang, W., Li, M. et al. (2015) A functional 4-hydroxybenzoate degradation pathway in the phytopathogen *Xanthomonas campestris* is required for full pathogenicity. *Scientific Reports*, 5, 18456.

Wargo, M.J. (2013) Homeostasis and catabolism of choline and glycine betaine: lessons from *Pseudomonas aeruginosa*. *Applied and Environmental Microbiology*, 79, 2112–2120.

Warnes, G., Bolker, B., Bonebakker, L., Gentleman, R., Huber, W., Liaw, A. et al. (2015) *gplots: Various R programming tools for plotting data*. R package version 3.0.1 Available at: https://CRAN.Rproject.org/package=gplots

Wengelnik, K., Rossier, O. & Bonas, U. (1999) Mutations in the regulatory gene *hrpG* of *Xanthomonas campestris* pv. *vesicatoria* result in constitutive expression of all *hrp* genes. *Journal of Bacteriology*, 181, 6828–6831.

Willsky, G.R. & Malamy, M.H. (1980) Characterization of two genetically separable inorganic phosphate transport systems in *Escherichia coli*. *Journal of Bacteriology*, 144, 356–365.

Yang, C., Huang, T.-W., Wen, S.-Y., Chang, C.-Y., Tsai, S.-F., Wu, W.-F. et al. (2012) Genome-wide PhoB binding and gene expression profiles reveal the hierarchical gene regulatory network of phosphate starvation in *Escherichia coli*. *PLoS One*, 7, e47314.

Zhang, F., Du, Z., Huang, L., Vera Cruz, C., Zhou, Y. & Li, Z. (2013) Comparative transcriptome profiling reveals different expression patterns in *Xanthomonas oryzae* pv. *oryzae* strains with putative virulence-relevant genes. *PLoS One*, 8, e64267.

Zhang, H.Y., Wei, J.W., Qian, W. & Deng, C.Y. (2020) Analysis of HrpG regulons and HrpG-interacting proteins by ChIP-seq and affinity proteomics in *Xanthomonas campestris*. *Molecular Plant Pathology*, 21, 388–400.

SUPPORTING INFORMATION

Additional supporting information may be found online in the Supporting Information section.

How to cite this article: Luneau, J.S., Cerutti, A., Roux, B., Carrère, S., Jardinaud, M.-F., Gaillac, A., et al. (2022) *Xanthomonas* transcriptome inside cauliflower hydathodes reveals bacterial virulence strategies and physiological adaptations at early infection stages. *Molecular Plant Pathology*, 23, 159–174. https://doi.org/10.1111/mpp.13117